



ELSEVIER

Contents lists available at ScienceDirect

## Biomedicine & Pharmacotherapy

journal homepage: [www.elsevier.com/locate/bioph](http://www.elsevier.com/locate/bioph)



### Cycloastragenol prevents age-related bone loss: Evidence in D-galactose-treated and aged rats

Yongjie Yu<sup>a,1</sup>, Jingkai Wu<sup>a,1</sup>, Jin Li<sup>a,1</sup>, Yanzhi Liu<sup>b,c</sup>, Xiaoyan Zheng<sup>a</sup>, Mingzhu Du<sup>a</sup>, Limin Zhou<sup>a</sup>, Yajun Yang<sup>a</sup>, Shiyong Luo<sup>a</sup>, Wenjia Hu<sup>d</sup>, Lin Li<sup>e</sup>, Weimin Yao<sup>f,\*</sup>, Yuyu Liu<sup>a,\*</sup>

<sup>a</sup> Department of Pharmacology, Guangdong Medical University, Zhanjiang, Guangdong, 524023, PR China

<sup>b</sup> Guangdong Key Laboratory for Research and Development of Natural Drugs, Marine Medical Research Institute, Guangdong Medical University, Zhanjiang, Guangdong, 524023, PR China

<sup>c</sup> Translational Medicine R&D Center, Institute of Biomedical and Health Engineering, Shenzhen Institutes of Advanced Technology, Chinese Academy of Sciences, Shenzhen, 518000, PR China

<sup>d</sup> Institute of Biochemistry and Molecular Biology, Guangdong Medical University, Zhanjiang, Guangdong, 524023, PR China

<sup>e</sup> Guangdong Provincial Key Laboratory of New Drug Screening, Guangzhou Key Laboratory of Drug Research for Emerging Virus Prevention and Treatment, School of Pharmaceutical Sciences, Southern Medical University, Guangzhou, Guangdong, 510515, PR China

<sup>f</sup> Department of Respiratory Medicine, The Affiliated Hospital of Guangdong Medical University, Zhanjiang, Guangdong, 524000, PR China

#### ABSTRACT

**Background and aims:** Aging-induced bone loss is a multifactorial, age-related, and progressive phenomenon among the general population and may further progress to osteoporosis and increase the risk of fractures. Cycloastragenol (CAG) currently the only compound reported that activates human telomerase, is thought to be able to alleviate or delay the symptoms of aging and chronic diseases. Previous research has suggested that CAG may have the potential to alleviate age-related bone loss. However, to date, no research has specifically focused on this aspect. In this study, we aimed to investigate whether CAG could prevent senile osteoporosis, and further reveal its underlying mechanism.

**Methods:** CAG treatment was administered into two bone loss rat models (D-galactose administration and aging) for 20 weeks and 33 weeks, respectively. Serum biomarkers analyses, bone biomechanical tests, micro-computed tomography assessment, and bone histomorphometry analyses were performed on the bone samples collected at the endpoint to determine whether CAG could prevent or alleviate age-related bone loss. Proteomic analysis was performed to reveal the changes in protein profiles of the bones, and western blot was used to further verify the identity of the key proteins. The viability, osteoblastic differentiation, and mineralization of MC3T3-E1 cells were also evaluated after CAG treatment *in vitro*.

**Results:** The results suggest that CAG treatment improves bone formation, reduces osteoclast number, alleviates the degradation of bone microstructure, and enhances bone biomechanical properties in both D-galactose- and aging-induced bone loss models. CAG treatment promotes viability, osteoblastic differentiation, and mineralization in MC3T3-E1 cells. Proteomic and western blot analyses revealed that CAG treatment increases osteoactivin (OA) expression to alleviate bone loss.

**Conclusion:** The results revealed that CAG alleviates age-related bone loss and improves bone microstructure and biomechanical properties. This may be due to CAG-induced increase in OA expression. In addition, the results support preclinical investigations of CAG as a potential therapeutic medicine for the treatment of senile osteoporosis.

#### ARTICLE INFO

**Keywords:** Cycloastragenol Aging, Osteoporosis, Osteoactivin

**Abbreviations:** CAG, cycloastragenol; D-Gal, D-galactose; OA, osteoactivin; SOP, senile osteoporosis; Micro-CT, micro-computed tomography; BV/TV, bone volume to total volume; Tb.N, trabecular number; Tb.Th, trabecular thickness; Tb.Sp, trabecular separation; E-%L.Pm, endosteum labeled perimeter percentage; P-%L.Pm, periosteum labeled perimeter percentage; BFR/TV, bone formation rate to total volume; MAR, mineral apposition rate; %Ob.Pm, osteoblast perimeter percentage; Oc.N, osteoclast number; DM, differentiation media

\* Corresponding authors.

E-mail addresses: [490296443@qq.com](mailto:490296443@qq.com) (W. Yao), [liuyuyu77@163.com](mailto:liuyuyu77@163.com) (Y. Liu).

<sup>1</sup> These authors contributed equally to this work.

<https://doi.org/10.1016/j.bioph.2020.110304>

Received 24 March 2020; Received in revised form 10 May 2020; Accepted 20 May 2020

0753-3322/© 2020 The Authors. Published by Elsevier Masson SAS. This is an open access article under the CC BY-NC-ND license (<http://creativecommons.org/licenses/by-nc-nd/4.0/>).

## 1. Introduction

Senile osteoporosis (SOP), a common skeletal disease closely associated with low quality of life among the aged population, is characterized by decreased osteoblast activity, low bone mass, and micro-architectural deterioration of bone tissue [1]. Senescent cells accumulate locally with aging, and components of the senescence-associated secretory phenotype (SASP) have deleterious autocrine and paracrine effects on bone [2]. These changes disturb the coupling balance between bone formation and resorption in bone remodeling, thereby leading to bone loss [3]. Telomere attrition is an important factor inducing senescence in bone, as it reduces the proliferation of bone cells [4], and decreases mesenchymal stem cells' (MSCs) differentiation into osteoblasts [5]. Another important trigger for senescence is increased oxidative stress, which has been reported to promote osteoclast activity and inhibit osteoblast function [6]. In addition, apoptosis of osteoblasts and osteocytes has been linked to increased levels of reactive oxygen species (ROS) [7]. With the growing aged population and increased life expectancy, SOP is becoming an increasingly difficult challenge for physicians. However, treatment of SOP relies on medications that were originally designed for post-menopausal osteoporosis. Although SOP is quite similar to post-menopausal osteoporosis, current medications do not specifically target the causal factor of the disease — aging [8,9].

Cycloastragenol (CAG), an aglycone of astragaloside IV isolated from *Astragalus membranaceus* Bunge, is the only compound known to activate human telomerase, to date [10]. Previous studies have reported that CAG has multiple pharmacological effects, including antioxidant [11], and anti-inflammation effects [12,13], promotion of autophagy [14], and improvement of lipid metabolism [15,16]. CAG has the potential to treat various diseases and prolong health span, possibly due to the activation of the MAPK, AMPK, or FXR signaling pathways [17].

Telomere attrition and oxidative stress are induce factor of aging [18]; thus, CAG is thought to alleviate or delay symptoms of aging and chronic diseases. Previous studies suggest that CAG may have the potential to alleviate age-related bone loss. However, to date, no study has specifically focused on this aspect. In this study, we aimed to investigate the preventive effects of CAG on age-related bone loss *in vitro* and *in vivo* using MC3T3-E1 cell model and D-galactose (D-Gal)-induced aging and natural aging rat models, respectively.

## 2. Materials and methods

### 2.1. Chemicals and reagents

Cycloastragenol was purchased from Best (Chengdu, China) (*in vitro* experiment) and Zelang Biological Technology (Nanjing, China) (*in vivo* experiment). D-galactose was purchased from Biosharp (Hefei, China). GPNMB polyclonal antibody was purchased from Thermo Fisher Scientific (Waltham, MA, USA). Beta-actin antibody was purchased from Cell Signaling Technology (Beverly, MA, USA).

### 2.2. Cell culture

MC3T3-E1 cells, obtain from the Anatomy Laboratory of Southern Medical University, were cultured in  $\alpha$ -MEM supplemented with 10 % FBS in a humidified atmosphere containing 5 % CO<sub>2</sub> at 37 °C. The medium was replaced every 3 days. When 80%–90% confluence was reached in the 25 mm culture bottle, cells were seeded in 96-well plates at a density of 3000 cells/well, in 24-well plates at a density of 5000 cells/well or in 12-well plates at a density of  $6 \times 10^4$  cells/well for different assays.

### 2.3. Cell viability assay

Viability of MC3T3-E1 cells were determined by a MTT kits as described previously [19]. MC3T3-E1 cells were plated in 96-well plates (3000 cells/well) and treated with different concentrations of CAG (0.03–3  $\mu$ M) and 10  $\mu$ M icariin. After culturing for 24, 48, and 72 h, viability was measured using MTT kit according to manufacturer's instruction (Nanjing Jiancheng, Nanjing, China).

### 2.4. Alkaline phosphatase (ALP) activity assay

MC3T3-E1 cells were seeded into 24-well plates (5000 cells/well) and treated with different concentrations of CAG (0.03–3  $\mu$ M) and 10  $\mu$ M icariin. After culturing for 5, 7, and 9 days, ALP activity assays were completed using ALP kit according to the manufacturer's instructions (Nanjing Jiancheng, Nanjing, China).

### 2.5. Cell mineralization assay

To determine calcium deposition, alizarin red staining was performed on day 7 to evaluate the mineralized matrix. Differentiation media (DM) was consisted of  $\alpha$ -MEM supplemented with 10 % FBS, 50  $\mu$ g/ml ascorbic acid and 10 mM  $\beta$ -glycerophosphate. Cells were divided into control, DM, 0.03  $\mu$ M CAG + DM, 0.1  $\mu$ M CAG + DM, 0.3  $\mu$ M CAG + DM and 10  $\mu$ M icariin + DM treatment cell groups. After culturing for 7 days, cells were stained with 0.1 % alizarin red (Sigma) at a pH of 7.2, and then examined *via* light microscopy.

### 2.6. Animals and experiment protocol

Male Sprague-Dawley rats were purchased from the Laboratory Animal Center of Southern Medical University. Female Sprague-Dawley rats were purchased from laboratory animal center of Guangxi Medical University. All mice were maintained under specific pathogen-free (SPF) conditions at Animal Center of Guangdong Medical University and approved by the local ethics authorities of Academic Committee on Ethics of Animal Experiments of the Guangdong Medical University, Zhanjiang, People's Republic of China.

D-galactose induced aging rat model: Fifty nine-week-old male Sprague-Dawley rats were randomly allocated to five group. A group was subcutaneously injected with D-Galactose (100 mg kg<sup>-1</sup>d<sup>-1</sup>) for 20 weeks. Three groups were administrated orally *via* gavage with CAG at dose 3, 7, or 14 mg kg<sup>-1</sup>d<sup>-1</sup>, for 20 consecutive weeks concurrent with D-galactose injection. In addition to a control group that received corresponding vehicles.

Natural aging rat model: Forty 51-week-old female Sprague-Dawley rats were randomly allocated to four groups. A group was administrated orally *via* gavage with corresponding vehicles for 33 consecutive weeks. Three groups were administrated orally *via* gavage with CAG at dose 3, 7, or 14 mg kg<sup>-1</sup>d<sup>-1</sup>, respectively, for 33 consecutive weeks. Eight 28-week-old female rats were set as control with no treatment.

### 2.7. ELISA

ELISA was performed to detect biomarkers in animal serum (TRACP, MDA) according to the manufacturer's instructions (Elabscience, Texas, USA).

### 2.8. Bone mechanical test

A three-point breaking test was performed on the midshaft of the right femurs obtained from all rats as previously described [20]. A Bose Electro Force Testing System (ELF3510; Bose Corp., Eden Prairie, MN, USA) was used. Bone samples were tested with a 1 mm indenter, at speed of 0.01 mm/s with 15 mm span.

## 2.9. Micro-computed tomography assessments (Micro-CT)

Micro CT analysis was performed as previously described [21]. The femur metaphyseal trabecular bones were scanned using vivaCT40 (Scanco Medical, Zurich, Switzerland) in high-resolution condition (X-ray energy on 70 KVp, 114  $\mu$ A, 8 W; integration time 200 ms). The region of interest was the distal femur metaphysis located between 1 and 4 mm distal to the growth plate epiphyseal junction.

## 2.10. Bone histomorphometry

Bone histomorphometry analyses were performed as previously described [22]. A semiautomatic digitizing image analysis system (Osteometrics, Inc., Decatur, GA, USA) was used for quantitative measurement. Undecalcified distal femur metaphysis and diaphysis were embedded in methacrylate, and 4 mm and 8 mm sections were cut. Unstained 8 mm sections were used to measure fluorescent calcein-labeled bone surfaces at a wavelength of 495 nm. For calcein labeling, rats were injected with 10 mg/kg body weight of green fluorescent Calcein (Sigma) at 3, 4, 13, and 14 days before sacrifice. Toluidine Blue staining was performed in 4 mm sections for quantification osteoblasts and osteoclasts.

## 2.11. Proteomic assay

Bone protein digestion was performed according to the FASP procedure [23], and the resulting peptide mixture was labeled using the TMT (Tandem mass tag) reagent according to the manufacturer's instructions (Thermo Scientific). TMT peptides were fractionated by SCX chromatography using the AKTA Purifier system (GE Healthcare). Liquid Chromatography (LC)-Electrospray Ionization (ESI) Tandem MS (MS/MS) was performed on a Q Exactive mass spectrometer that was coupled to Easy nLC (Proxeon Biosystems, now Thermo Fisher Scientific). MS/MS spectra were searched using MASCOT engine (Matrix Science, London, UK; version 2.2) embedded into Proteome Discoverer 1.3 (Thermo Electron, San Jose, ca.) against Ensemble\_Rat (Database) and the decoy database.

## 2.12. Western blotting

Bones were snap-frozen in liquid nitrogen, grounded into powder, and lysed in RIPA buffer [24]. Protein extracts were separated on 10 % SDS polyacrylamide gel, transferred on polyvinylidene fluoride membranes, and stained with antibodies against the indicated primary antibodies.

## 2.13. Statistical analysis

Data were collected from experiments and expressed as the mean  $\pm$  standard deviation. The statistical differences were analyzed by one-way analysis of variance with Least Significant Difference and Student-Newman-Keuls post hoc tests using SPSS 19.0 software (IBM Corp., Armonk, NY, USA). In proteomic analysis, statistical differences were analyzed by Fisher's exact test.  $P < 0.05$  was considered to indicate a statistically significant difference.

## 3. Results

### 3.1. CAG has no effect on the body weight of rats

Free radical theory is a classical theory of aging [25]. Excessive doses of D-galactose resulted in large amounts of ROS and galactitol, impairing cell function and eventually leading to aging [26]. D-galactose-induced aging models share a lot in common with the natural aging model. However, natural aging is more complicated. Therefore, both the D-galactose-treated and the natural aging model rats were used

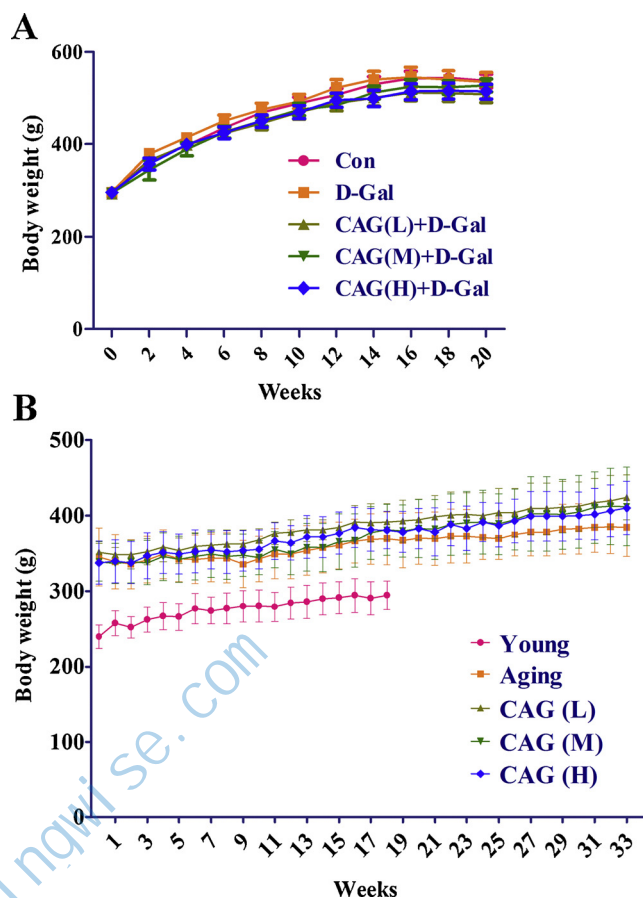


Fig. 1. Effects of CAG on body weight of rats.

(A) Body weights of rats in the D-galactose-treated model were determined every two weeks. Treatment started from the second week and lasted until the 20th week. (B) Body weights of rats in the aged model were determined on a weekly basis. Treatment started from the second week and lasted until the 33rd week.

Abbreviation: D-Gal, D-galactose; CAG(L), low dose of CAG; CAG(M), medium dose of CAG; CAG(H), high dose of CAG.

to evaluate the effect of CAG on age-related bone loss. No significant differences in body weight and behavior were noted in the two models throughout the experimental period (Fig. 1A and B).

### 3.2. CAG decreases serum bone resorption marker in D-Gal-treated rats

D-Gal-treated rats exhibited increased serum bone resorption marker (TRACP) levels by 101 % compared to vehicle-treated rats, and a 79.5 % increase in oxidative stress marker (MDA) levels, showing no significant difference. The elevation in TRACP levels was inhibited by low (L), medium (M), and high (H) doses of CAG treatment by 20.5 %, 17 %, and 17 %, respectively (Fig. 2A). CAG(L), CAG(M), and CAG(H) also resulted in 59 %, 69 %, and 51 % decrease in levels of MDA, respectively, but the differences of CAG(H) were not statistically significant ( $P = 0.051$ ) (Fig. 2B). Serum biomarkers analysis suggested that CAG treatment inhibits bone resorption and improve oxidative stress.

### 3.3. CAG protects from bone strength decline

Bone fractures are closely related to the biomechanical properties of bone. Rats treated with D-Gal for 20 weeks exhibited a 12 % decrease in both the rigidity coefficient (indicative of structure strength) and the maximum load (indicative of structure strength and apparent material strength), compared to vehicle-treated rats; CAG treatment inhibited

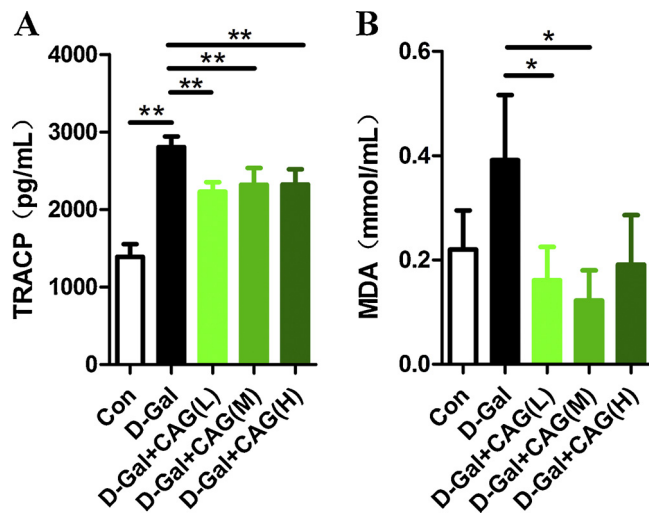


**Fig. 2.** Effect of CAG on serum TRACP and MDA levels in d-Gal-treated rats. Serum levels of (A) TRACP (n = 8 for each group) and (B) MDA (n = 7–10 for each group) in d-Gal-treated rats. All data are presented as means ± standard deviation. \*P < 0.05; \*\*P < 0.01 (one-way analysis of variance). Abbreviation: TRACP, tartrate resistant acid phosphatase; MDA, malondialdehyde; d-Gal, d-galactose; CAG(L), low dose of CAG; CAG(M), medium dose of CAG; CAG(H), high dose of CAG.

the reduction in bone strength. CAG(L) treatment improved the rigidity coefficient by 14.5 %. CAG(H) treatment improved the rigidity coefficient and maximum load by 13 % and 14 %, respectively (Fig. 3A–C).

Aged rats treated with CAG for 33 weeks showed improved bone strength. CAG(L)-treated aged rats showed increased maximum and elastic load by 15 % and 20 %, respectively, compared to vehicle-treated aged rats (Fig. 3D–F). Three-point bending tests suggested that CAG treatment resulted in improved bone strength in the aging model rats.

### 3.4. CAG protects against bone loss

To verify the preventive influence of CAG on age-related bone loss, we scanned trabecular bone using a micro-CT machine and reconstructed a 3D-image of the bone microstructure. d-Gal-treated rats showed a 19 % decrease in trabecular number (Tb.N) and a 38 % increase in trabecular separation (Tb.Sp) compared to vehicle-treated rats. The decline in trabecular bone microstructure was inhibited by CAG treatment. CAG(L) treatment caused a 26 % increase in Tb.N, a 27 % increase in bone mineral density (BMD), and a 30.5 % decrease in Tb.Sp. CAG(M) treatment caused a 23 % increase in Tb.N and a 28 % decrease in Tb.Sp (Fig. 4A and Table 1).

Aged rats exhibited decreases in bone mass (BV/TV), Tb.N, trabecular thickness (Tb.Th), and BMD by 65 %, 54 %, 26 %, and 34 %, respectively, Tb.Sp increased by 221.5 %, compared to young rats. These changes were attenuated by CAG treatment. Both CAG(L) and

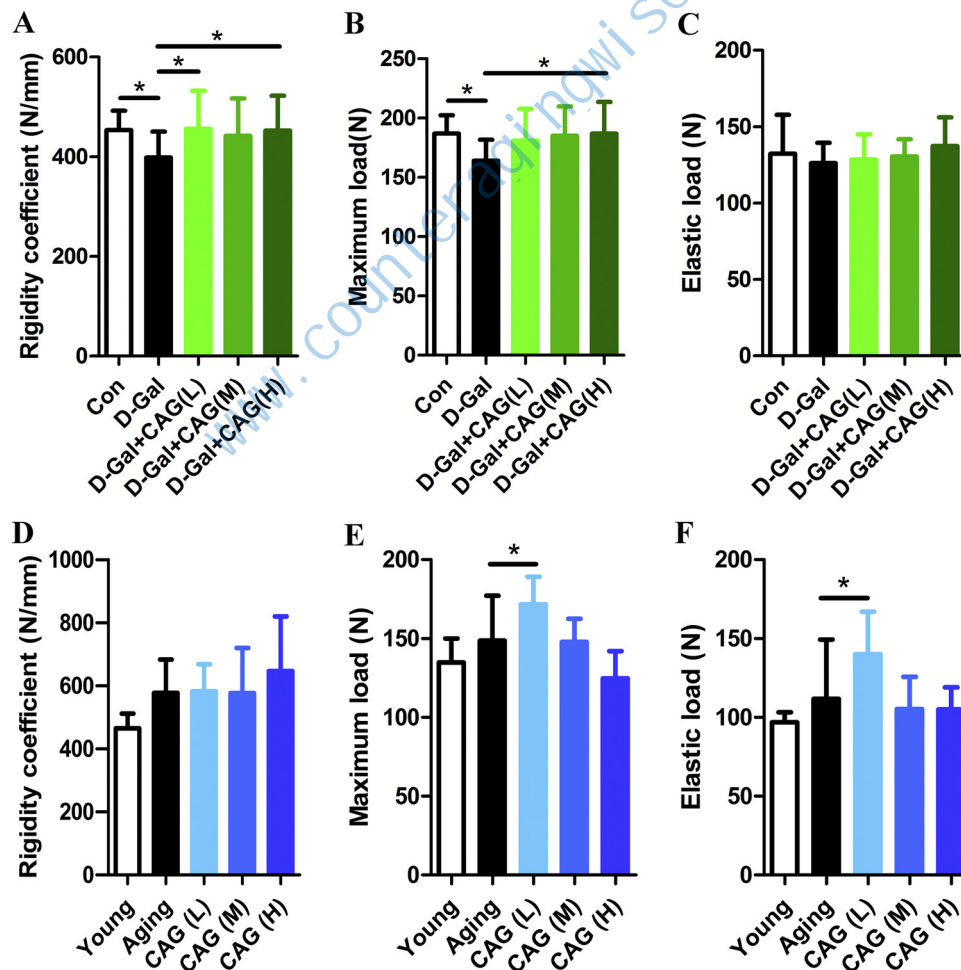


**Fig. 3.** CAG treatment improves bone biomechanical properties in d-Gal-treated and aged rats. Quantification of three-point bending test-derived rigidity coefficient, maximum load, and elastic load on (A–C) d-Gal-treated rats (n = 8 for each group) and (D–F) aged rats (n = 6–9 for each group). All data are presented as means ± standard deviation. \*P < 0.05 (one-way analysis of variance). Abbreviation: N, newton; d-Gal, d-galactose; CAG(L), low dose of CAG; CAG(M), medium dose of CAG; CAG(H), high dose of CAG.



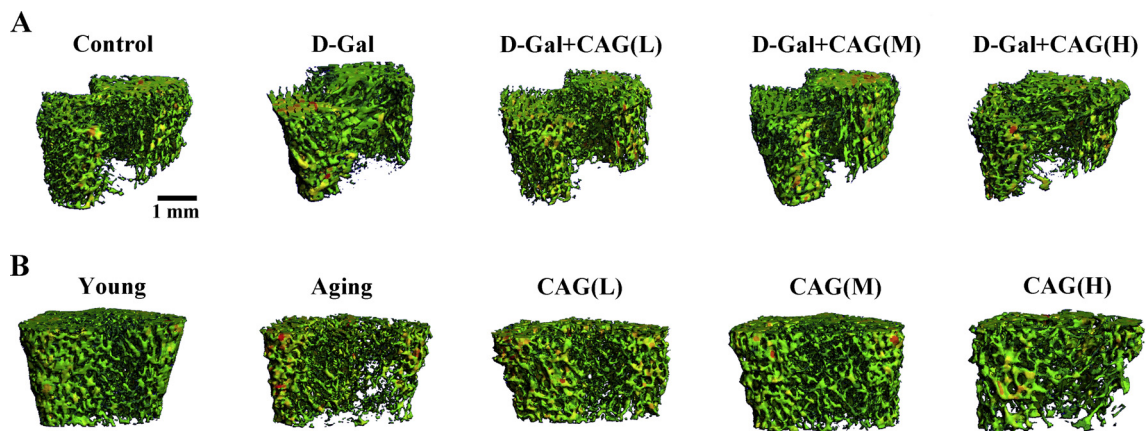


Fig. 4. CAG alleviates age-related bone loss in D-Gal-treated and aged rats.

Representative micro-computed tomography (Micro-CT) images of bone microarchitecture in the femur metaphyseal of (A) D-galactose-treated rats ( $n = 8$  for each group) and (B) aged rats ( $n = 6-9$  for each group).

Abbreviation: D-Gal, D-galactose; CAG(L), low dose of CAG; CAG(M), medium dose of CAG; CAG(H), high dose of CAG.

CAG(M) treatment resulted in a 19 % increase in Tb.Th (Fig. 4B and Table 2). Micro-CT assay showed that CAG treatment resulted in better trabecular bone microarchitecture in aging model rats.

CAG-treated rats had higher bone mass (BV/TV) in both aging models (47 % by CAG(L) in D-Gal-treated rats and 71 % by CAG(M) in aged rats), but the differences were not statistically significant.

### 3.5. CAG reduces osteoclast number and improves bone formation

Bone histomorphometry analysis was performed on the femur metaphysis and tibia diaphysis to determine whether the protective effect of CAG on bones is related to the restoration of bone formation and inhibition of bone resorption in aging rats. D-Gal-treated rats showed a 497 % decrease in bone formation (BFR/TV), a 55 % decrease in mineral apposition rate (MAR), and a 46 % increase in osteoclast number (Oc.N), compared to vehicle-treated rats; these changes were inhibited by CAG treatment. CAG(L) and CAG(H) treatments increased BFR/TV by 251 % and 273 %, respectively. CAG(H) treatment increased MAR by 125 %. CAG(L), CAG(M), and CAG(H) treatments decreased Oc.N by 28.5 %, 28.5 %, and 34.3 %, respectively (Fig. 5A and Table 3).

Aged rats exhibited a 27 % increase in Oc.N, a 46 % decrease in osteoblast activity (%Ob.Pm), and a 63 % decrease in BFR/TV, compared to young rats. CAG(L) treatment decreased Oc.N by 83 %. CAG(M) treatment increased %Ob.Pm by 45 %, however, this difference was not statistically significant (Fig. 5B and Table 4). In the tibia metaphysis, bone histomorphometry results suggested that CAG treatment reduced osteoclast number.

Rats treated with D-Gal and CAG showed an increase in bone formation parameter (E-%L.Pm) compared to rats treated with only D-Gal, however, these results were not statistically significant (Fig. 6A and C).

Compared to aged rats treated with vehicle, aged rats treated with CAG(L) and CAG(H) exhibited a 114 % and 123 % increase in bone

formation parameter (P-%L.Pm), respectively (Figure 6B and D). In the femur diaphysis, bone histomorphometry results indicate that CAG treatment improves diaphysis bone formation.

The aforementioned results suggest that CAG treatment reduces osteoclast number (tibia metaphysis) and improves bone formation (femur diaphysis).

### 3.6. OA is related to the prevention of bone loss by CAG

We further aimed to elucidate the underlying mechanism of the preventive effects of CAG on age-related bone loss. Bone proteins from young rats, aged rats, and CAG(M)-treated aged rats were collected and used for proteomic analyses. Results showed that CAG(M)-treated aged rats had 26 up-regulated proteins and 54 down-regulated proteins, compared to aged rats (Fig. 7A). We focused on proteins linked to bone metabolism. One of these proteins, osteoactivin (OA), has previously been reported to promote osteogenic differentiation, improve bone formation [27,28], and inhibit osteoclast differentiation [29]. Proteomic analysis showed that CAG(M) treatment increases OA expression (Figure 7B), similar results were observed in the western blot analysis (Figure 7C and D). Together, this indicates that CAG-mediated prevention of age-related bone loss may be attributed to increased OA expression.

### 3.7. CAG exerts pro-osteogenic effect in pre-osteoblasts

Osteoblastic MC3T3-E1 cells are similar to primary calvarial osteoblasts, thus they are a good model for studying osteogenic activity [30]. Icarin has been reported to effectively enhance proliferation and osteogenesis of bone marrow mesenchymal stem cells; therefore, it was used as the positive control for this experiment [31]. MC3T3-E1 cells treated with CAG showed increased viability, osteoblastic

Table 1

Micro-CT analysis of femur metaphyseal trabecular bone in D-Gal-treated rats.

Parameters	Groups				
	Control	D-Gal	CAG(L)+D-Gal	CAG(M)+D-Gal	CAG(H)+D-Gal
BV/TV/%	0.21 ± 0.03	0.17 ± 0.07	0.25 ± 0.09	0.22 ± 0.08	0.21 ± 0.06
Tb.N/mm <sup>-1</sup>	3.08 ± 0.28	2.50 ± 0.65*	3.16 ± 0.49 <sup>#</sup>	3.08 ± 0.54 <sup>#</sup>	2.90 ± 0.43
Tb.Th/mm	0.07 ± 0.005	0.07 ± 0.014	0.08 ± 0.016	0.07 ± 0.014	0.07 ± 0.009
Tb.Sp/mm	0.26 ± 0.03	0.36 ± 0.15*	0.25 ± 0.07 <sup>#</sup>	0.26 ± 0.07 <sup>#</sup>	0.28 ± 0.06
BMD/mg* cm <sup>-3</sup>	298.25 ± 7.09	274.38 ± 39.29	349.28 ± 39.18 <sup>#</sup>	297.34 ± 54.80	312.59 ± 41.72

All data are presented as means ± standard deviation ( $n = 8$  for each group). \*  $P < 0.05$  vs Control; <sup>#</sup>  $P < 0.05$  vs D-Gal (one-way analysis of variance).

Abbreviation: BV/TV, bone volume to total volume; Tb.N, trabecular number; Tb.Th, trabecular thickness; Tb.Sp, trabecular separation; BMD, bone mineral density.

**Table 2**  
Micro-CT analysis of femur metaphyseal trabecular bone in aged rats.

Parameters	Groups				
	Young	Aging	CAG(L)	CAG(M)	CAG(H)
BV/TV/%	0.318 ± 0.06	0.111 ± 0.56*	0.167 ± 0.07	0.19 ± 0.1	0.149 ± 0.09
Tb.N/mm <sup>-1</sup>	4.39 ± 0.49	2.03 ± 0.75*	2.55 ± 0.7	2.86 ± 1.2	2.26 ± 0.86
Tb.Th/mm	0.072 ± 0.007	0.053 ± 0.01*	0.063 ± 0.013 <sup>#</sup>	0.063 ± 0.009 <sup>#</sup>	0.062 ± 0.013
Tb.Sp/mm	0.158 ± 0.03	0.508 ± 0.22*	0.365 ± 0.17	0.356 ± 0.2	0.424 ± 0.16
BMD/mg*cm <sup>-3</sup>	326.2 ± 36.33	214 ± 56.37*	244.6 ± 57.07	267.6 ± 94.19	228.8 ± 79.76

All data are presented as means ± standard deviation (n = 6–9 for each group). \*  $P < 0.05$  vs Young; <sup>#</sup>  $P < 0.05$  vs Aging (one-way analysis of variance). Abbreviation: BV/TV, bone volume to total volume; Tb.N, trabecular number; Tb.Th, trabecular thickness; Tb.Sp, trabecular separation; BMD, bone mineral density.

differentiation (ALP activity), and mineralization (mineralized nodule) in a dose- and time-dependent manner (from 0.03  $\mu\text{M}$ –0.3  $\mu\text{M}$ ). Cells treated with CAG at 0.03  $\mu\text{M}$  for 48 h had better viability (Fig. 8A), and cells treated with CAG at 0.03  $\mu\text{M}$  for seven days had higher ALP activity, compared to cells treated with icariin (Figure 8B). Moreover, the effect of 0.3  $\mu\text{M}$  CAG on mineralization was comparable to that of 10  $\mu\text{M}$  icariin (Figure 8C). These results suggest that CAG has the capacity to enhance bone formation.

#### 4. Discussion

According to previous studies, an increase in SOP causes a significant elevation in the occurrence of bone fractures, and up to 25 % of elderly hip fracture patients die within a year of injury [32,33]. Fear of serious adverse side effects in hormone replacement therapy and anti-resorptive therapy has significantly diminished patient compliance [34]. Thus, there is a need for new therapeutic approaches, with less adverse side effects and higher efficacy. The present study provides a new therapeutic option for senile osteoporosis. Results indicated that both D-Gal treatment and natural aging in rats lead to bone loss via degradation of the trabecular bone microstructure and decline in bone biomechanical properties. Supplementation with CAG was shown to improve skeletal phenotype in two age-related bone loss models. Results demonstrated that CAG supplementation leads to lower bone resorption, while bone formation remains unchanged in the tibia metaphysis, thereby maintaining bone mass and bone microarchitecture. In addition, CAG improves the bone formation of femur diaphysis, thereby enhancing bone biomechanical properties. Furthermore, our results suggest that CAG potentially prevents age-related bone loss by increasing osteostatin (OA) expression.

OA, a type I transmembrane glycoprotein, is known to be vital in bone formation. There are numerous cells within the skeletal system that express OA, including osteoblasts, osteoclasts, macrophages, and

dendritic cells. Exogenous treatment with recombinant OA significantly enhanced the osteogenic differentiation potential of MSCs [35]. Moreover, OA plays an important role in bone metabolism *in vivo* by promoting bone formation and inhibiting bone resorption [27,28]. Proteomic analysis showed that OA expression was up-regulated in aged rats treated with CAG at 7 mg kg<sup>-1</sup>d<sup>-1</sup>, this was further supported by western blot analysis. To the best of our knowledge, the present study is the first to report that the effects of CAG on preventing age-related bone loss may be attributed to the regulation of OA expression. Further studies are needed to elucidate the relationship between the anti-osteoporotic effects of CAG and OA.

In this study, we used two different aging rat models: D-Gal-induced aging model [36] and natural aging model [37]. D-Gal-induced aging animal model, based on the free radical theory, has been widely accepted in previous research. In the present study, rats treated with D-Gal for 20 weeks exhibited a decline in bone biomechanical properties and a degradation in bone microstructure, following decreased bone formation activity and increased osteoclast number. These changes were significantly alleviated by CAG treatment. CAG treatment at a dose of 3, 7, or 14 mg kg<sup>-1</sup>d<sup>-1</sup> decreased serum bone resorption marker (TRACP) levels, serum oxidative stress marker (MDA) levels, and osteoclast number. Simultaneously, it also increased bone formation activity and BMD. CAG facilitates osteoblast mineralization *in vitro*; this is consistent with *in vivo* BMD data. The effects of CAG may contribute to improvement in the biomechanical properties and microstructure of bones.

Aging is a complex and gradual process characterized by cellular senescence. Inducers of senescence include telomere dysfunction, reactive oxygen species, chromatin alterations, DNA damage, and oncogene activation [38]. Bone remodeling is disrupted by senescent cells and their secreted factors, leading to a decline in bone formation and an elevation in resorption, ultimately causing osteoporosis [39]. In the present study, 84-week-old rats demonstrated degraded bone

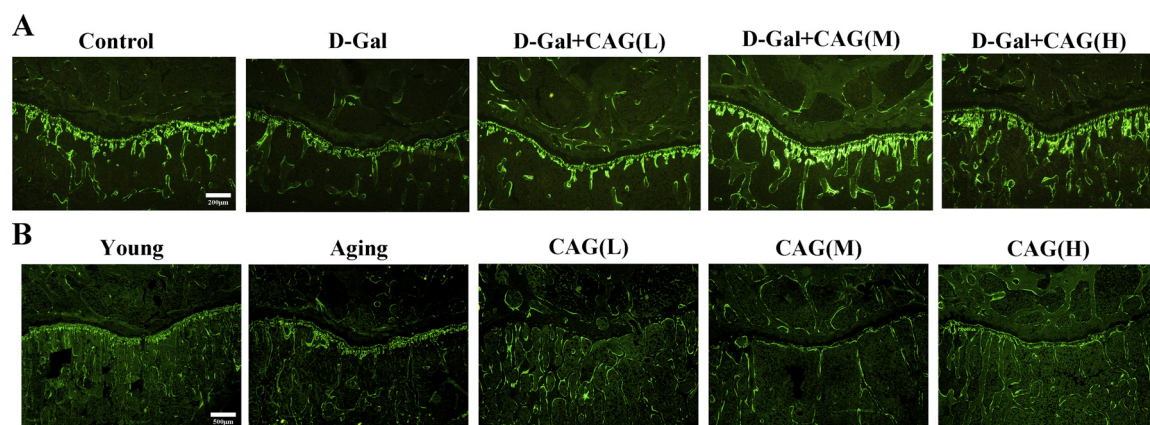


**Fig. 5.** Effect of CAG on bone formation decline in the tibial metaphysis.

Representative fluorescence micrographs of the tibial metaphysis of (A) D-Gal-treated rats (n = 8 for each group) and (B) aged rats (n = 6–9 for each group). Abbreviation: D-Gal, D-galactose; CAG(L), low dose of CAG; CAG(M), medium dose of CAG; CAG(H), high dose of CAG.

**Table 3**  
Histomorphological analysis of proximal tibial metaphysis in D-Gal-treated rats.

Parameters	Groups Control	D-Gal	CAG(L) +D-Gal	CAG(M) +D-Gal	CAG(H) +D-Gal
BFR/TV(%/year)	117.34 ± 50.43	19.60 ± 10.26**	68.76 ± 59.14 <sup>#</sup>	39.42 ± 34.80	73.57 ± 38.31 <sup>#</sup>
MAR(μm/d)	2.04 ± 0.73	0.91 ± 0.41**	1.54 ± 0.63	1.23 ± 0.42	2.05 ± 0.57 <sup>#</sup>
%Ob.Pm(%)	1.71 ± 0.32	1.37 ± 0.59	1.81 ± 0.73	1.90 ± 0.34	1.56 ± 0.55
Oc.N(no.mm)	0.24 ± 0.14	0.35 ± 0.06*	0.25 ± 0.11 <sup>#</sup>	0.25 ± 0.06 <sup>#</sup>	0.23 ± 0.08 <sup>#</sup>

All data are presented as means ± standard deviation (n = 8 for each group). \**P* < 0.05, \*\**P* < 0.01 vs Control; <sup>#</sup>*P* < 0.05 vs D-Gal (one-way analysis of variance). Abbreviation: BFR/TV, bone formation rate to total volume; MAR, mineral apposition rate; %Ob.Pm, osteoblast perimeter percentage; Oc.N, osteoclast number.

**Table 4**  
Histomorphological analysis of proximal tibial metaphysis in aged rats.

Parameters	Groups Young	Aging	CAG(L)	CAG(M)	CAG(H)
BFR/TV(%/year)	127.5 ± 21.2	47.59 ± 30.2*	46.56 ± 24.8	35.63 ± 19.1	45.57 ± 21.1
MAR(μm/d)	1.41 ± 0.23	1.13 ± 0.49	1.15 ± 0.13	1.12 ± 0.21	1.35 ± 0.71
%Ob.Pm(%)	0.339 ± 0.186	0.184 ± 0.112*	0.184 ± 0.14	0.266 ± 0.273	0.249 ± 0.127
Oc.N(no.mm)	1.13 ± 1.25	1.44 ± 1.01*	0.25 ± 0.46 <sup>#</sup>	0.78 ± 1.09	1.67 ± 1.21

All data are presented as means ± standard deviation (n = 6–9 for each group). \**P* < 0.05, \*\**P* < 0.01 vs Young; <sup>#</sup>*P* < 0.05 vs Aging (one-way analysis of variance). Abbreviation: BFR/TV, bone formation rate to total volume; MAR, mineral apposition rate; %Ob.Pm, osteoblast perimeter percentage; Oc.N, osteoclast number.

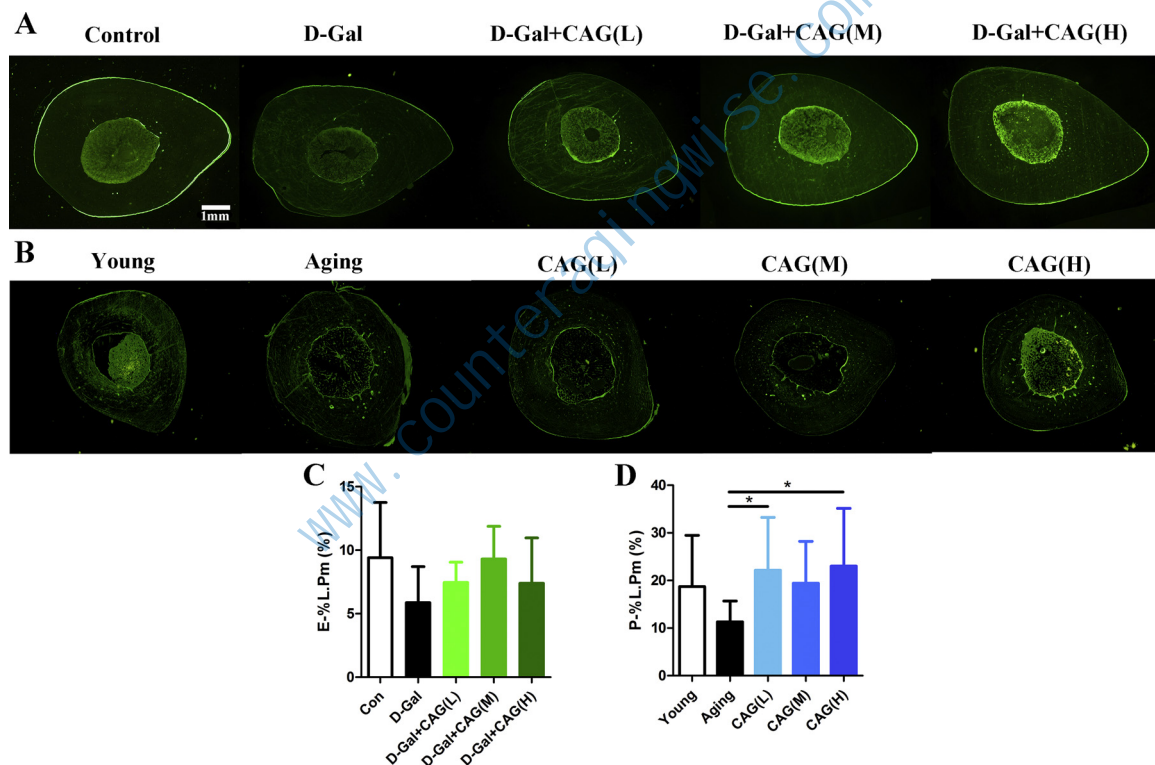


**Fig. 6.** CAG alleviates bone formation decline in the tibial diaphysis. Representative fluorescence micrographs of the tibial diaphysis of (A) D-Gal-treated rats and (B) aged rats. (C) Quantification of E-%L.Pm in the tibial diaphysis of D-Gal-treated rats (n = 8 for each group). (E) Quantification of P-%L.Pm in the tibial diaphysis of aged rats (n = 6–9 for each group). All data are presented as means ± standard deviation. \**P* < 0.05 (one-way analysis of variance). Abbreviation: D-Gal, D-galactose; CAG(L), low dose of CAG; CAG(M), medium dose of CAG; CAG(H), high dose of CAG; E-%L.Pm, endosteum labeled perimeter percentage; P-%L.Pm, periosteum labeled perimeter percentage.

microstructure, increased osteoclast number, and decreased bone formation. These changes could be alleviated by CAG treatment. Treatment with CAG for 33 weeks led to a decrease in osteoclast number (tibia metaphysis) and an improvement in bone formation (femur diaphysis). These effects may contribute to the increased trabecular bone thickness and enhanced bone biomechanical properties in aged rats. The results from both the aging rat models demonstrated that CAG

treatment was able to alleviate age-related bone loss.

Duration is a major obstacle in aging research, but it could be solved by using an inducing agent [40]. Our data suggests that D-Gal-treated rats and aged rats exhibited similar bone loss, impaired bone microarchitecture, and altered bone metabolism; only a small difference was found between these two models. Trabecular bone thickness showed no decrease in D-Gal-treated rats, whereas it decreased in aged rats. CAG



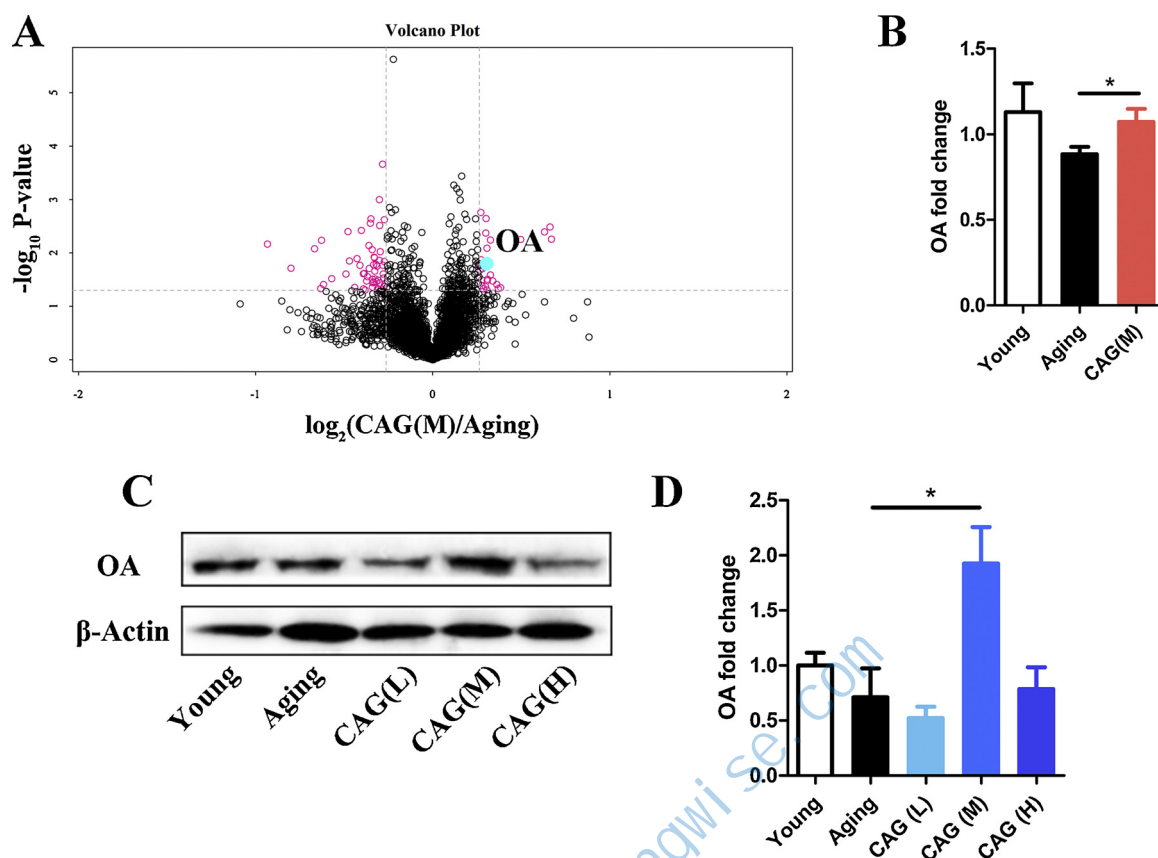


**Fig. 7.** CAG increases osteoactivin expression.

Proteomic analysis showed that osteoactivin (OA) was up-regulated in CAG(M)-treated aged rats. (A) Volcano plot showing that CAG-treated rats had increased OA expression compared to aged rats. (B) Quantification of change in OA expression level. (C) Western blot analysis further proves that OA was up-regulated after CAG treatment, and (D) quantification of that change. All data are presented as means  $\pm$  standard deviation. \* $P < 0.05$  (Fisher's exact test in proteomic analysis; One-way analysis of variance in western blot analysis).

Abbreviation: OA, osteoactivin; CAG(L), low dose of CAG; CAG(M), medium dose of CAG; CAG(H), high dose of CAG.

was shown to cause greater improvement in preventing bone loss in D-Gal-treated rats than in aged rats. Excess D-Gal is converted into aldose and hydroperoxide through the catalyzation of galactose oxidase, resulting in the generation of ROS which subsequently causes oxidative stress, inflammation, mitochondrial dysfunction, telomere attrition, and apoptosis, eventually leading to aging; thus, a drug-induced aging model is more rapid and stable. However, at least ten hallmarks and more than five inducers are involved in the natural aging process, and overexpression of ROS is just one of these [18]. This may explain the small difference observed between the D-Gal-induced aging model and the natural aging rat model, as natural aging involves more complex mechanisms. Taken together, our data suggest that the D-Gal-induced aging model is suitable for testing the effect of compounds on age-related bone loss. However, this model does not fully represent bone loss in the natural aging process.

Notably, incubation of pre-osteoblasts with high concentrations of CAG (3  $\mu\text{M}$ ) for up to 72 h did not impair cell viability. The dose of CAG used in this study (daily oral gavage for up to 33 weeks) did not cause any adverse behavioral events or abnormal changes in bone histology and body weight during the entire duration of the study, suggesting that CAG has a safe profile; consistent with published literature [41]. The safety of the compound demonstrated in the study provides a proof of concept for the feasibility of CAG treatment for clinical transformation.

Senescent cells have a negative effect on bones in the long run. Genetic or pharmacological approaches to clear senescent cells result in better skeletal phenotypes in aged mice. Similar results were observed when factors secreted by senescent cells (senescence-associated secretory phenotype) were inhibited. Clearing senescent cells resulted in

lower bone resorption and either an increase (cortical bone) or maintenance (trabecular bone) in bone formation [42]. Similar bone metabolism changes were found in aging rat models in the present study after CAG treatment. Aging is a gradual process which may be rescued by pharmacological treatment [43]. Although it is beyond the scope of the present study, it would be interesting to examine whether CAG has an effect on reducing senescent cell formation by activating telomerases, which may be an alternative option for clearing senescent cells.

In summary, our results revealed that CAG alleviates age-related bone loss, improves bone microstructure and biomechanical properties. This is potentially due to CAG-induced increase in osteoactivin expression. Furthermore, our results support preclinical investigations of CAG as a potential therapeutic medicine for the treatment of senile osteoporosis.

#### Declaration of Competing Interest

The authors declare that there are no conflicts of interest.

#### Acknowledgments

This study was supported by the National Natural Science Foundation of China (No. 81703584), Guangdong Province Natural Science Foundation of China (No.2017A030310614), China Postdoctoral Science Foundation (2018M633192), and the Scientific Research Foundation for PhD of Guangdong Medical University (No: B2017030).



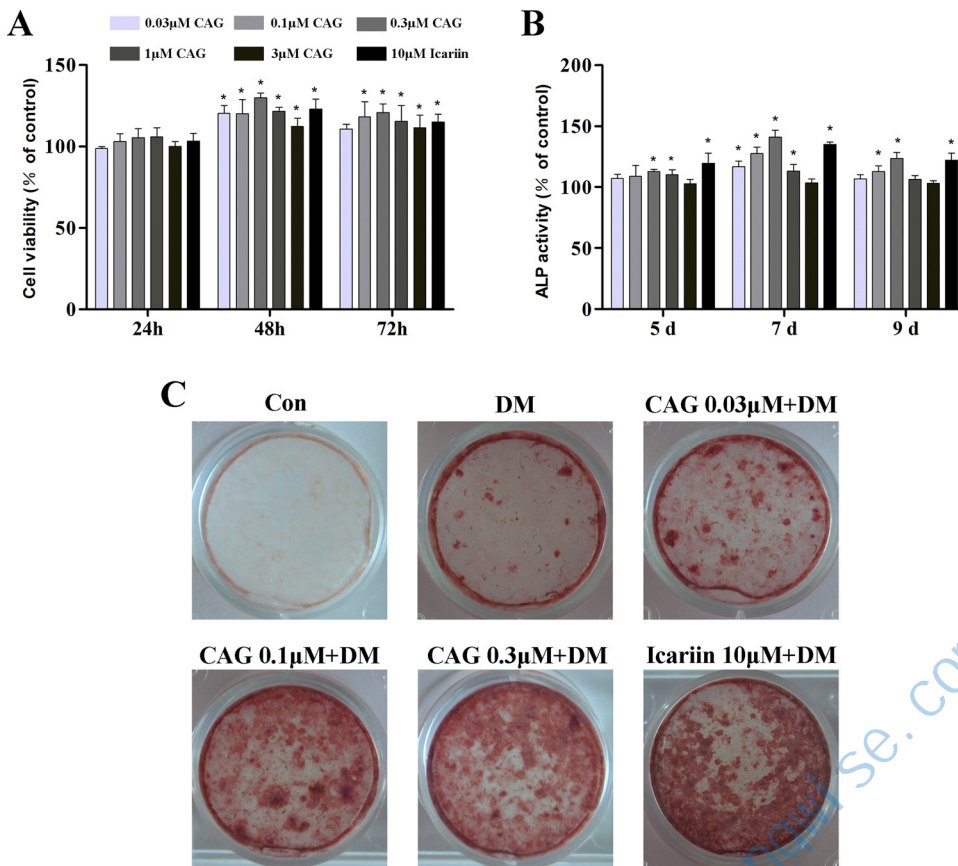


**Fig. 8.** CAG improves viability, osteoblastic differentiation, and mineralization in MC3T3-E1 cells.

(A) Cell viability, (B) osteoblastic differentiation, and (C) mineralization were measured in MC3T3-E1 cells. Icaritin-treated group was set as the positive control. All data are presented as means  $\pm$  standard deviation. \* $P < 0.05$  (one-way analysis of variance).

Abbreviation: ALP, alkaline phosphatase; DM, differentiation media.

## Appendix A. Supplementary data

Supplementary material related to this article can be found, in the online version, at doi:<https://doi.org/10.1016/j.biopha.2020.110304>.

## References

- [1] A.Y. Bijlsma, C.G.M. Meskers, R.G.J. Westendorp, A.B. Maier, Chronology of age-related disease definitions: osteoporosis and sarcopenia, *Ageing Res. Rev.* 11 (2) (2012) 320–324, <https://doi.org/10.1016/j.arr.2012.01.001>.
- [2] P.D. Saville, Osteoporosis: disease or senescence? *Lancet.* 1 (7541) (1968) 535, [https://doi.org/10.1016/s0140-6736\(68\)91510-9](https://doi.org/10.1016/s0140-6736(68)91510-9).
- [3] A.M. Parfitt, The coupling of bone formation to bone resorption: a critical analysis of the concept and of its relevance to the pathogenesis of osteoporosis, *Metab. Bone Dis. Relat. Res.* 4 (1) (1982) 1–6, [https://doi.org/10.1016/0221-8747\(82\)90002-9](https://doi.org/10.1016/0221-8747(82)90002-9).
- [4] H. Saeed, B.M. Abdallah, N. Ditzel, P. Catala-Lehnen, W. Qiu, M. Amling, et al., Telomerase-deficient mice exhibit bone loss owing to defects in osteoblasts and increased osteoclastogenesis by inflammatory microenvironment, *J. Bone Miner. Res.* 26 (7) (2011) 1494–1505, <https://doi.org/10.1002/jbmr.349>.
- [5] Robert J. Pignolo, Robin K. Suda, Emily A. McMillan, Johnny Shen, Seoung-Hoon Lee, Yongwon Choi, et al., Defects in telomere maintenance molecules impair osteoblast differentiation and promote osteoporosis, *Aging Cell* 7 (1) (2008) 23–31, <https://doi.org/10.1111/j.1474-9726.2007.00350.x>.
- [6] I.R. Garrett, B.F. Boyce, R.O. Oreffo, L. Bonewald, J. Poser, G.R. Mundy, Oxygen-derived free radicals stimulate osteoclastic bone resorption in rodent bone in vitro and in vivo, *J. Clin. Invest.* 85 (3) (1990) 632–639, <https://doi.org/10.1172/jci114485>.
- [7] K.H. Baek, K.W. Oh, W.Y. Lee, S.S. Lee, M.K. Kim, H.S. Kwon, et al., Association of oxidative stress with postmenopausal osteoporosis and the effects of hydrogen peroxide on osteoclast formation in human bone marrow cell cultures, *Calcif. Tissue Int.* 87 (3) (2010) 226–235, <https://doi.org/10.1007/s00223-010-9393-9>.
- [8] E. Baum, K.M. Peters, The diagnosis and treatment of primary osteoporosis according to current guidelines, *Arztebl. Int.* 105 (33) (2008) 573–582, <https://doi.org/10.3238/arztebl.2008.0573>.
- [9] J. Compston, A. Cooper, C. Cooper, N. Gittoes, C. Gregson, N. Harvey, et al., UK clinical guideline for the prevention and treatment of osteoporosis, *Arch. Osteoporos.* 12 (1) (2017) 43, <https://doi.org/10.1007/s11657-017-0324-5>.
- [10] L. Salvador, G. Singaravelu, C.B. Harley, P. Flom, A. Suram, J.M. Raffaele, A natural product telomerase activator lengthens telomeres in humans: a randomized, double blind, and placebo controlled study, *Rejuvenation Res.* 19 (6) (2016) 478–484, <https://doi.org/10.1089/rej.2015.1793>.
- [11] Y. Wang, C. Chen, Q. Wang, Y. Cao, L. Xu, R. Qi, Inhibitory effects of cycloastragenol on abdominal aortic aneurysm and its related mechanisms, *Br. J. Pharmacol.* 176 (2) (2019) 282–296, <https://doi.org/10.1111/bph.14515>.
- [12] Y. Zhao, Q. Li, W. Zhao, J. Li, Y. Sun, K. Liu, et al., Astragaloside IV and cycloastragenol are equally effective in inhibition of endoplasmic reticulum stress-associated TXNIP/NLRP3 inflammasome activation in the endothelium, *J. Ethnopharmacol.* 169 (2015) 210–218, <https://doi.org/10.1016/j.jep.2015.04.030>.
- [13] C. Sun, M. Jiang, L. Zhang, J. Yang, G. Zhang, B. Du, et al., Cycloastragenol mediates activation and proliferation suppression in concanavalin A-induced mouse lymphocyte pan-activation model, *Immunopharmacol. Immunotoxicol.* 39 (3) (2017) 131–139, <https://doi.org/10.1080/08923973.2017.1300170>.
- [14] J. Wang, M.L. Wu, S.P. Cao, H. Cai, Z.M. Zhao, Y.H. Song, Cycloastragenol ameliorates experimental heart damage in rats by promoting myocardial autophagy via inhibition of AKT1-RPS6KB1 signaling, *Biomed. Pharmacother.* 107 (2018) 1074–1081, <https://doi.org/10.1016/j.biopha.2018.08.016>.
- [15] S. Wang, C. Zhai, Q. Liu, X. Wang, Z. Ren, Y. Zhang, et al., Cycloastragenol, a triterpene aglycone derived from *Radix astragalii*, suppresses the accumulation of cytoplasmic lipid droplet in 3T3-L1 adipocytes, *Biochem. Biophys. Res. Commun.* 450 (1) (2014) 306–311, <https://doi.org/10.1016/j.bbrc.2014.05.117>.
- [16] M. Gu, S. Zhang, Y. Zhao, J. Huang, Y. Wang, Y. Li, et al., Cycloastragenol improves hepatic steatosis by activating farnesoid X receptor signaling, *Pharmacol. Res.* 121 (2017) 22–32, <https://doi.org/10.1016/j.phrs.2017.04.021>.
- [17] Y. Yu, L. Zhou, Y. Yang, Y. Liu, Cycloastragenol: an exciting novel candidate for age-associated diseases, *Exp. Ther. Med.* 16 (3) (2018) 3175–3182, <https://doi.org/10.3892/etm.2018.6501>.
- [18] C. López-Otin, M.A. Blasco, L. Partridge, M. Serrano, G. Kroemer, The hallmarks of aging, *Cell* 153 (6) (2013) 1194–1217, <https://doi.org/10.1016/j.cell.2013.05.039>.
- [19] Y. Zheng, J. Li, J. Wu, Y. Yu, W. Yao, M. Zhou, et al., Tetrahydroxystilbene glucoside isolated from *Polygonum multiflorum* Thunb. demonstrates osteoblast differentiation promoting activity, *Exp. Ther. Med.* 14 (4) (2017) 2845–2852, <https://doi.org/10.3892/etm.2017.4915>.
- [20] S. Lin, J. Huang, L. Zheng, L. Zheng, Y. Liu, G. Liu, et al., Glucocorticoid-induced osteoporosis in growing rats, *Calcif. Tissue Int.* 95 (4) (2014) 362–373, <https://doi.org/10.1007/s00223-014-9899-7>.
- [21] Y. Liu, Y. Cui, X. Zhang, X. Gao, Y. Su, Bilian Xu, et al., Effects of salvinolate on bone metabolism in glucocorticoid-treated lupus-prone B6.MRL-Fas (lpr) /J mice, *Drug Des. Devel. Ther.* 10 (2016) 2535–2546, <https://doi.org/10.2147/dddt.s110125>.
- [22] L. Cui, T. Li, Y. Liu, L. Zhou, P. Li, B. Xu, Salvanolic acid B prevents bone loss in prednisone-treated rats through stimulation of osteogenesis and bone marrow angiogenesis, *PLoS One* 7 (4) (2012) e34647, <https://doi.org/10.1371/journal.pone.0034647>.
- [23] J.R. Wisniewski, A. Zougman, N. Nagaraj, M. Mann, Universal sample preparation

- method for proteome analysis, *Nat. Methods* 6 (5) (2009) 359–362, <https://doi.org/10.1038/nmeth.1322>.
- [24] Y. Yang, Y. Su, D. Wang, Y. Chen, Y. Liu, S. Luo, et al., Tanshinol rescues the impaired bone formation elicited by glucocorticoid involved in KLF15 pathway, *Oxid. Med. Cell. Longev.* 2016 (2016) 1092746, <https://doi.org/10.1155/2016/1092746>.
- [25] K.B. Beckman, B.N. Ames, The free radical theory of aging matures, *Physiol. Rev.* 78 (2) (1998) 547–581, <https://doi.org/10.1152/physrev.1998.78.2.547>.
- [26] Y.T. Hung, M.A. Tikhonova, S.J. Ding, P.F. Kao, H.H. Lan, J.M. Liao, Effects of chronic treatment with diosgenin on bone loss in a D-galactose-induced aging rat model, *Chin. J. Physiol.* 57 (3) (2014) 121–127, <https://doi.org/10.4077/cjp.2014.bac199>.
- [27] S.M. Abdelmagid, J.Y. Belcher, F.M. Moussa, S.L. Lababidi, G.R. Sondag, K.M. Novak, et al., Mutation in osteoactivin decreases bone formation in vivo and osteoblast differentiation in vitro, *Am. J. Pathol.* 184 (3) (2014) 697–713, <https://doi.org/10.1016/j.ajpath.2013.11.031>.
- [28] N. Frara, S.M. Abdelmagid, G.R. Sondag, Fouad M. Moussa, Vanessa R. Yingling, et al., Transgenic expression of osteoactivin/gpnmh enhances bone formation in vivo and osteoprogenitor differentiation ex vivo, *J. Cell. Physiol.* 231 (1) (2016) 72–83, <https://doi.org/10.1002/jcp.25020>.
- [29] S.M. Abdelmagid, G.R. Sondag, F.M. Moussa, J.Y. Belcher, B. Yu, H. Stinnett, et al., Mutation in Osteoactivin promotes receptor activator of NFκB ligand (RANKL)-mediated osteoclast differentiation and survival but inhibits osteoclast function, *J. Biol. Chem.* 290 (33) (2015) 20128–20146, <https://doi.org/10.1074/jbc.m114.624270>.
- [30] D. Wang, K. Christensen, K. Chawla, G. Xiao, P.H. Krebsbach, R.T. Franceschi, Isolation and characterization of MC3T3-E1 preosteoblast subclones with distinct in vitro and in vivo differentiation/mineralization potential, *J. Bone Miner. Res.* 14 (6) (1999) 893–903, <https://doi.org/10.1359/jbmr.1999.14.6.893>.
- [31] Xiaoxiao Liang, Zhiqiang Hou, Yuanlong Xie, Feifei Yan, Sisi Li, Xiaobin Zhu, et al., Icaritin promotes osteogenic differentiation of bone marrow stromal cells and prevents bone loss in OVX mice via activating autophagy, *J. Cell. Biochem.* 120 (8) (2019) 13121–13132, <https://doi.org/10.1002/jcb.28585>.
- [32] N.C. Wright, A.C. Looker, K.G. Saag, J.R. Curtis, E.S. Delzell, S. Randall, et al., The recent prevalence of osteoporosis and low bone mass in the United States based on bone mineral density at the femoral neck or lumbar spine, *J. Bone Miner. Res.* 29 (11) (2014) 2520–2526, <https://doi.org/10.1002/jbmr.2269>.
- [33] R. Burge, B. Dawson-Hughes, D.H. Solomon, J.B. Wong, A. King, A. Tosteson, Incidence and economic burden of osteoporosis-related fractures in the United States, 2005–2025, *J. Bone Miner. Res.* 22 (3) (2007) 465–475, <https://doi.org/10.1359/jbmr.061113>.
- [34] S. Khosla, E. Shane, A crisis in the treatment of osteoporosis, *J. Bone Miner. Res.* 31 (8) (2016) 1485–1487, <https://doi.org/10.1002/jbmr.2888>.
- [35] X. Hu, P. Zhang, Z. Xu, H. Chen, X. Xie, GPNMB enhances bone regeneration by promoting angiogenesis and osteogenesis: potential role for tissue engineering bone, *J. Cell. Biochem.* 114 (2) (2013) 2729–2737, <https://doi.org/10.1002/jcb.24621>.
- [36] J. Long, X. Wang, H. Gao, Z. Liu, C.S. Liu, M.Y. Mao, et al., D-galactose toxicity in mice is associated with mitochondrial dysfunction: protecting effects of mitochondrial nutrient R-alpha-lipoic acid, *Biogerontology*. 8 (3) (2007) 373–381, <https://doi.org/10.1007/s10522-007-9081-y>.
- [37] V.L. Ferguson, R.A. Ayers, T.A. Bateman, S.J. Simske, Bone development and age-related bone loss in male C57BL/6J mice, *Bone* 33 (3) (2003) 387–398, [https://doi.org/10.1016/s8756-3282\(03\)00199-6](https://doi.org/10.1016/s8756-3282(03)00199-6).
- [38] R.J. Pignolo, R.M. Samsonraj, S.F. Law, H. Wang, A. Chandra, Targeting cell senescence for the treatment of age-related bone loss, *Curr. Osteoporos. Rep.* 17 (2) (2019) 70–85, <https://doi.org/10.1007/s11914-019-00504-2>.
- [39] J.N. Farr, S. Khosla, Cellular senescence in bone, *Bone* 121 (2019) 121–133, <https://doi.org/10.1016/j.bone.2019.01.015>.
- [40] K.F. Azman, R. Zakaria, D-Galactose-induced accelerated aging model: an overview, *Biogerontology* 20 (6) (2019) 763–782, <https://doi.org/10.1007/s10522-019-09837-y>.
- [41] N.J. Szabo, Dietary safety of cycloastragenol from *Astragalus* spp.: subchronic toxicity and genotoxicity studies, *Food Chem. Toxicol.* 64 (2014) 322–334, <https://doi.org/10.1016/j.fct.2013.11.041>.
- [42] J.N. Farr, M. Xu, M.M. Weivoda, D.G. Monroe, D.G. Fraser, J.L. Onken, et al., Targeting cellular senescence prevents age-related bone loss in mice, *Nat. Med.* 23 (9) (2017) 1072–1079, <https://doi.org/10.1038/nm.4385>.
- [43] C.D. Wiley, J. Campisi, From ancient pathways to aging cells-connecting metabolism and cellular senescence, *Cell Metab.* 23 (6) (2016) 1013–1021, <https://doi.org/10.1016/j.cmet.2016.05.010>.